© 2026. Published by The Company of Biologists | Journal of Experimental Biology (2026) 229, jeb251920. doi:10.1242/jeb.251920

RESEARCH ARTICLE

Buoyancy regulation through modulation of onboard gas volume by resting sperm whales (*Physeter macrocephalus*)

Noémie Freymond[1,2,*], Alec Burslem[1] and Patrick J. O. Miller[1]

ABSTRACT

Sperm whales rest while drifting under the surface in a unique stereotypical vertical position. This position is thought to enable them to sleep effectively by buffering them from surface wave action, while avoiding the costs of transiting to deeper depths. While resting, sperm whales release bubbles, hypothesised to help them regulate their buoyancy. As sperm whales are breath-hold divers, if they slowly drift up while resting, the gas in their lung will slowly expand following Boyle–Mariotte's gas law. Hence, releasing bubbles would enable them to counteract the expanding diving gas and achieve neutral buoyancy. To test this hypothesis and examine how buoyancy influences resting sperm whales, we created a simulation based on tissue density, drag coefficient and onboard gas volume, and matched it to depth profiles from 10 of 42 tagged individuals in Norway that rested primarily by diving head-down. All individuals resting during such dives released bubbles, and the results from the simulation confirmed that release of bubbles functioned to regulate their buoyancy to remain submerged while resting. Additionally, the results indicate that sperm whales start resting dives with less diving gas volume than for deep foraging dives. These results demonstrate that sperm whales actively regulate their buoyancy while resting by releasing bubbles and adjusting their initial diving gas volume. We cannot rule out the possibility that releasing bubbles is related to the offgassing of excess CO_2 or N_2 from tissues into the lungs, so this behaviour could also have implications for metabolic gas exchange.

KEY WORDS: Sleep, Resting dives, Bubbles, Biologging data, Biomechanics

INTRODUCTION

Sleep can be defined as a behavioural state that fulfils four criteria: (1) a specific posture, (2) quiescence, (3) reduced responsiveness to external stimuli, and (4) rapid reversibility to wakefulness given sufficient stimulation (Flanigan, 1972; Piéron, 1913). Sleep can also be defined using electrophysiological correlates associated with behaviourally defined sleep. Although several physiological parameters differ between sleep and wakefulness, electroencephalogram (EEG) changes have received the most attention. Despite being relatively well studied in captive toothed whales, sleep remains poorly understood in larger free-ranging whales. Most studies on sleep have been conducted on small captive marine mammals, on which an EEG could be performed. Although recent technological improvements have enabled the recording of brain activity in free-ranging northern elephant seals (*Mirounga angustirostris*) and minke whales (*Balaenoptera acutorostrata*) (Kendall-Bar et al., 2023; Houser et al., 2024), these recordings involved, respectively, anaesthetising and handling the individuals, approaches that are currently not feasible for larger whale species. When EEG cannot be used, the detection of sleep relies on behavioural criteria, such as those described by Piéron (1913). Visual observation of sleeping behaviour is challenging because of the need to monitor a 24 h time frame. This challenge can be addressed using biologging tags equipped with accelerometers, allowing fine-scale movement data collection over extended periods, ranging from hours to days.

Sperm whales rest in a stereotypical vertical position, drifting under the surface (Miller et al., 2008). This position is thought to buffer them from surface wave action. While drifting in this stereotypical position, sperm whales showed reduced responsiveness to the close proximity of boats, in contrasts to their usual response while horizontally logging, and only reacted once touched by the boat, reflecting rapid state reversibility (Miller et al., 2008). This behaviour, hence, fulfils the behavioural criteria of sleep, namely a specific posture (which facilitates detection of resting in tag records) (Isojunno and Miller, 2015), quiescence, reduced responsiveness and rapid reversibility (Piéron, 1913). However, unlike for other smaller toothed cetaceans that can be studied in captivity, the brain activity of resting sperm whales has not been measured via an EEG. Consequently, in this study this behaviour will be referred to as resting rather than sleep.

Sperm whales initiate resting dives in two different ways (Miller et al., 2008). They either let the posterior part of their body sink, directly leading to a head-up position ('head-up resting'), or they first dive head-down before reversing into a head-up position ('head-down/head-up resting'). When first diving head-down, the whales have previously been shown to reach depths of 16.5±4.9 m, shielding the resting whale from surface wave action (Miller et al., 2008). The rotation to a head-up position is thought to occur passively, driven by low-density organs located in the anterior part of their bodies (e.g. lungs, respiratory tract and spermaceti organ; Miller et al., 2008, Clarke, 1978). In addition, Isojunno and Miller (2015) described another resting behaviour, in which whales drifted passively upward after a foraging dive ('deep drifting resting'). Sound recordings of resting sperm whales identified the occurrence of bubble releases, which were hypothesised to help sperm whales regulate their buoyancy while resting (Miller et al., 2004, 2008; Movie 1).

In the present study, we aimed to: (1) describe the underwater resting behaviour of sperm whales, (2) detail the bubble releases happening during resting periods, and (3) investigate the influence of buoyancy forces on their resting behaviour, testing whether bubble releases help sperm whales regulate their buoyancy. To test this hypothesis, we created a simulation to derive depth profiles of resting individuals based on varying amounts of onboard gas, and

[1]Sea Mammal Research Unit, Scottish Oceans Institute, School of Biology, University of St Andrews, St Andrews, Fife KY16 8LB, UK. [2]Université de Neuchâtel, Institut de Biologie, Rue Emile-Argand 11, 2000 Neuchâtel, Switzerland.

*Author for correspondence (noemie.freymond@gmail.com)

N.F., 0009-0000-9814-8289; A.B., 0000-0001-7591-8391

Received 15 November 2025; Accepted 15 May 2026

Journal of Experimental Biology (2026) 229, jeb251920. doi:10.1242/jeb.251920

compared simulated profiles with empirical data collected by biologging tags.

Net buoyancy is proportional to the difference in density between an animal's body and the surrounding medium. Animals denser than the surrounding seawater sink, whereas those with lower density float upward. In addition to net buoyancy, moving animals are also affected by drag forces, which oppose the direction of movement and increase with the speed of the animal (Fig. 1A). In the case of breath-hold divers, such as sperm whales, total body density is influenced by the combination of the density of their non-gaseous tissue (tissue density) and the volume of diving gases they carry in their lungs and acoustic apparatus (Miller et al., 2004). The influence of carried gas decreases with depth, as diving gas volumes compress under hydrostatic pressure according to Boyle's law (Fig. 1B). Tissue density is largely determined by the ratio of adipose to lean tissue of animals, as lipids are less dense than other tissue constituents (Moya-Laraño et al., 2008). Consequently, individuals with greater proportions of lipids will have more buoyant tissues than leaner individuals (Webb et al., 1998). Variation in net buoyancy has been shown to modulate the stroking and gliding pattern of swimmers and the rate of drift during passive drifting dives (Miller et al., 2004; Biuw et al., 2003).

Because of the substantial influence of buoyancy forces, aquatic animals have developed strategies to regulate their net buoyancy. For instance, teleost fish adjust the gas content of their swim bladder, while king penguins (*Aptenodytes patagonicus*) and Adélie penguins (*Pygoscelis adeliae*) modify their gas volume before diving (Arnold and Geer Walker, 1992; Sato et al., 2002). Resting sperm whales would benefit from neutral buoyancy to maintain their position in the water column without expending energy, and we hypothesise that bubble releases help them achieve this. As sperm whales drift upward after their body rotates to a head-up orientation (Miller et al., 2008), the diving gas volume in their lung will expand as a result of decreasing hydrostatic pressure, resulting in continued ascent to the surface (Fig. 1B; Boyle–Mariotte's gas law). Active regulation of buoyancy through bubble releases (detectable on tag sound recordings) would help them counteract the expanding diving gas underwater, enabling prolonged periods of rest.

MATERIALS AND METHODS

Data collection

Biologging data from 42 sperm whale tag deployments were used. The deployments took place in Northern Norway (a foraging ground for sexually segregated male North Atlantic sperm whales), in the region of the Lofoten Islands, between 69.0–70.5° northern latitude and 13.0–18.0° eastern latitude, and the data collection took place during eight boreal summers between 2005 and 2019. Free-ranging sperm whales, *Physeter macrocephalus* Linnaeus 1758, were tagged opportunistically using a pole from a small tag boat. Individuals were tagged with audio- and movement-recording data loggers, called Dtags (Johnson, Aguilar de Soto and Madsen, 2009), equipped with suction cups. These Dtags contained stereo hydrophones, pressure and temperature sensors, and a 3-axis accelerometer and 3-axis magnetometer. During the 2008 to 2019 field seasons, conductivity, temperature and depth (CTD) casts were also taken (for detailed methods, see Miller et al., 2011; Lam et al., 2018a,b; Kvadsheim et al., 2020; Teloni et al., 2008).

All field procedures involving sperm whales were approved by the Animal Welfare Ethics Committee at the University of St Andrews, and permitted by the Norwegian Animal Research Authority.

Data processing

Audio data were sampled at 96 kHz while movement sensor data were sampled at 50 Hz. Movement sensor data were then reduced to a sampling rate of 5 Hz and used to calculate the depth, acceleration and pitch (Johnson and Tyack, 2003; Miller et al., 2011, 2012). Where available, CTD casts were converted to seawater density using the standard international thermodynamic equation of state for seawater (Millero, 2010). During the 2016 deployments, only temperature casts were recorded. In order to estimate seawater density, temperature profiles were used, with salinity extrapolated

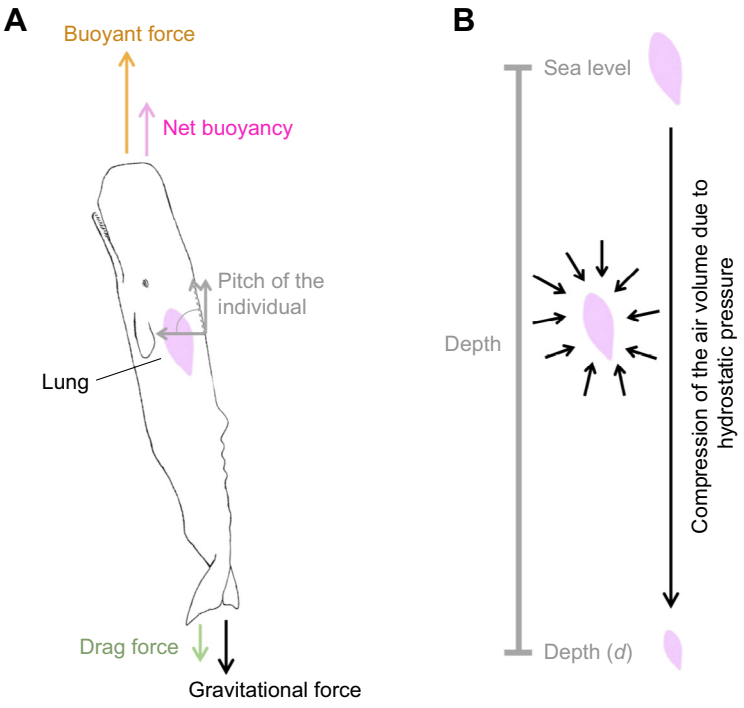

Fig. 1. Forces acting on resting sperm whales. (A) Illustration of the forces acting on a drifting whale. The buoyant force, directed upward, arises from the displacement of seawater by the body. The gravitational force, directed downward, is proportional to the mass of the individual, equivalent to its volume multiplied by the density of all tissue and air components. The net buoyancy is the difference between buoyant and the gravitational forces. In this schematic diagram, buoyant force exceeds gravitational force, resulting in positive net buoyancy. The drag force opposes the direction of movement; as the whale moves upward, the drag force is directed downward. The pitch angle indicates the inclination of the body, with an absolute value of pitch of 90 deg representing a vertical position. (B) Illustration of Boyle–Mariotte's gas law, showing the compression of the air carried by the whale at depth due to hydrostatic pressure.

from 2017 CTD casts (see Lam et al., 2018a,b). Deployments from 2005 were excluded from analysis as no CTD cast was recorded.

Data analysis

Identification of resting periods

Resting periods can be detected using depth and pitch data, as typical resting periods have a near-vertical pitch and a shallow depth. In order to detect these periods consistently, a hidden state model developed by Isojunno and Miller (2015) was used; only resting periods longer than 5 min were included in the analyses. Moreover, during some resting periods, there were periods of high pitch instability, which were not considered resting by the model. Periods of instability within resting periods of up to 2 min were still included in the resting dive, while longer periods were excluded from the analysis. Only resting dives that started with a head-down orientation were used for further analyses. Head-up resting dives were shallow enough for the head of the whale to potentially break the water surface, which would violate a key assumption of our modelling that the whole body is submerged and subject to buoyancy forces. Moreover, in such cases, the blowhole of the whale may not be immersed, which could make bubble releases inaudible.

Acoustic detection of bubble releases

For each resting period, acoustic recordings were inspected both aurally and visually using the 'tagaudit' and 'd3audit' function from the DTAG MATLAB toolbox (spectrogram frequency range: 0–3 kHz, time span: 7 s; https://soundtags.wp.st-andrews.ac.uk/dtags/dtag-toolbox/) (The MathWorks Inc., https://www.mathworks.com). For each bubble release event, the start and the end of the release were noted and a quality score was assigned (see Appendix: 'Bubble auditing'). Only bubble releases that were classified with high confidence were included in downstream analyses. The bubble releases varied in both duration and intensity, as indicated by the colour on the spectrogram showing the intensity of the sound (Fig. 2).

Simulation of the physical forces acting upon a resting sperm whale

The simulation aimed to integrate the external forces acting on a resting sperm whale to investigate their influence on the resting behaviour and whether bubble releases can help sperm whales regulate their net buoyancy. In order to mimic the depth profile of a resting sperm whale, two physical equations describing the motion of an object under constant acceleration were used (Eqns 1 and 2):

$$v = v_0 + at, \tag{1}$$

$$x = \frac{1}{2}at^2 + v_0t + x_0, \tag{2}$$

where v_0 and x_0 correspond respectively to the velocity and position at time t=0, v and x correspond to the velocity and position at any later time t, and a corresponds to the acceleration at a time t. In our case, the position (x) corresponds to the depth of the individual, and velocity (v) and acceleration (a) refer to the vertical vector. The vertical velocity of the resting individuals was calculated as the change in depth between each 0.2 s interval and transformed into metres per second. A symmetric filter impulse response (FIR) filter was subsequently used to filter the background noise from the vertical velocity.

An estimation of the acceleration of the whale was needed to simulate vertical speed and position (Eqns 1 and 2). The acceleration of a passive individual is mainly affected by two forces: hydrodynamic drag and net buoyancy (Fig. 1A). The hydrodynamic performance equation from Miller et al. (2016), which is simplified in Eqn 4, describes the acceleration of a gliding whale according to these two forces. The equation is derived from Newton's second law, describing that force (F) is equal to the mass (m) of the object multiplied by its acceleration (a) (Eqn 3):

$$F = m \cdot a. \tag{3}$$

In the case of a passively drifting individual, the acceleration is calculated as the sum of the drag and the net buoyancy divided by the mass of the individual (Eqn 4):

$$a = \frac{-F_{\text{Drag}} + F_{\text{Net buoyancy}}}{m}. \tag{4}$$

Eqn 4 was combined with Eqns 1 and 2 to estimate the velocity, depth and acceleration at each time step of 0.2 s. Acceleration was assumed to be constant within each 0.2 s interval.

Eqn 5 shows a slightly modified version of the hydrodynamic performance equation from Miller et al. (2016), with the abbreviations and their units explained in Table 1. The modification of the equation concerns the pitch (p) present in the second and third additive terms (Eqn 5, 'Influence of tissue density' and 'Influence of air carried in the lung'), which relates to the influence of net buoyancy on acceleration (Miller et al., 2016). A drifting individual is expected to move vertically regardless of its body orientation, as seen in the drifting model elaborated by Biuw et al. (2003). As a result, the sine of pitch was removed and replaced by the pitch angle divided by the absolute value of the pitch. Negative pitch values indicate a head-down position, while positive ones reflect a head-up position. Hence, dividing the pitch by its absolute value provides the direction

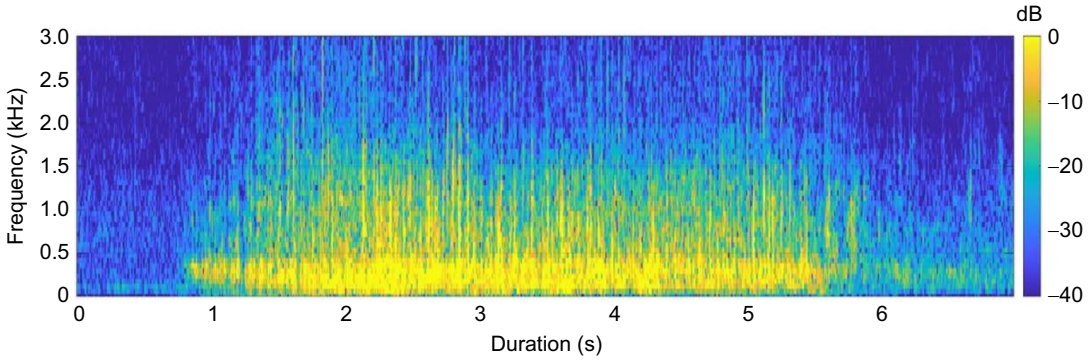

Fig. 2. Example spectrogram of a loud release of bubbles. The typical frequency was between 0 and 3 kHz, with a stronger intensity than the background noise, as shown by the yellow colour. The colour bar indicates the relative intensity of the sound in decibels (dB).

Journal of Experimental Biology (2026) 229, jeb251920. doi:10.1242/jeb.251920

Table 1. Description of the abbreviations and their units used in the hydrodynamic performance equation (Eqn 5)

Variable	Description	Units
a	Acceleration	m s^{-2}
A	Surface area	m^2
C_d	Drag coefficient	unitless
d	Depth	m
$\boldsymbol{g}$	Gravitational constant (9.80665 m s^{-2})	m s^{-2}
m	Mass	kg
p	Pitch angle	rad
ρ_{air}	Gas density	kg m^{-3}
ρ_{sw}	Seawater density	kg m^{-3}
ρ_{tissue}	Tissue density	kg m^{-3}
v	Speed	m s^{-1}
V_{air}	Volume of diving gas	ml

of net buoyancy:

$$a = \overbrace{-\frac{1}{2}\cdot\frac{C_d\cdot A}{m}\cdot\rho_{sw}\cdot v^2}^{\text{Drag force}} + \overbrace{\left(\frac{\rho_{sw}}{\rho_{tissue}}-1\right)\cdot\boldsymbol{g}\cdot\frac{p}{\text{abs}(p)}}^{\text{Influence of tissue density}} + \overbrace{\frac{V_{air}}{m}\cdot\boldsymbol{g}\cdot\frac{p}{\text{abs}(p)}\cdot\frac{(\rho_{sw}-(\rho_{air}\cdot(1+0.1\cdot d)))}{(1+0.1\cdot d)}}^{\text{Influence of air carried in the lung}}. \quad (5)$$

The first additive term of Eqn 5 ('Drag force') describes the influence of hydrodynamic drag on acceleration. Drag always opposes the motion of any moving object and is proportional to the square of speed (v), the passive drag coefficient (C_d) and the individual's surface area (A). C_d for sperm whales was estimated to be 0.003 by Miller et al. (2004).

The second and third additive terms of Eqn 5 ('Influence of tissue density' and 'Influence of air carried in the lung') relate to the influence of net buoyancy on the acceleration of the whale. Net buoyancy corresponds to the difference between buoyant and gravitational forces (Fig. 1A) and determines whether the animal will rise or sink. The critical aspect determining net buoyancy is the overall body density; for breath-hold divers, net buoyancy is treated separately into two parts: the influence of non-gaseous tissue and the diving gas carried by the whale.

The second additive term of Eqn 5 ('Influence of tissue density') relates to the influence of the whale's non-gaseous tissue (ρ_{tissue}). A whale's tissue density reflects its proportion of lipids, which varies between individuals. The magnitude of the influence of the tissue density depends on the surrounding seawater density (ρ_{sw}). Sperm whale tissue is expected to be relatively incompressible compared with the diving gas carried in the lung (Miller et al., 2004). However, substantial depths are expected to compress this tissue. As some deep drifting resting dives exceeded 300 m in depth, the tissue density was adjusted for the compressibility encountered at depth (see Appendix, Eqn A2; Miller et al., 2016).

Finally, the third term of Eqn 5 ('Influence of air carried in the lung') represents the influence of the gases carried by the whale on net buoyancy. This influence is greatly affected by depth (d), as individuals are subject to hydrostatic pressure. The initial gas volume at the surface (V_{air}) and diving gas density (ρ_{air}) were adjusted for the increased hydrostatic pressure at depth following Boyle–Mariotte's gas law.

Implementation of the simulation

The simulation was implemented in the R programming environment (https://www.r-project.org/). The hydrodynamic performance equation (Eqn 5) and the equation for velocity and position (Eqns 1 and 2) were combined in the simulation. The simulation aimed to mimic the depth profile of a resting whale as a time series with 0.2 s intervals (matching the 5 Hz sampling rate of the biologging data). Biologging data were integrated into the simulation in the form of initial conditions, making the simulation a hybrid model that compared observed depth data with simulated outcomes.

To account for differences in density between animals not attributable to differences in diving gas volumes, estimates of each individual tissue density were needed. Tissue density estimates were obtained using the hydrodynamic performance equation (see Appendix, Eqn A1; Miller et al., 2016). This method estimates several parameters based on the acceleration of gliding individuals, namely initial diving gas volume (V_{air}), tissue density (ρ_{tissue}) and the drag coefficient (C_d). These different parameters were estimated at the individual and population level using a Bayesian approach (Miller et al., 2016). The estimates were obtained based on gliding periods of 5 s occurring at depths greater than 100 m. The coefficients were, therefore, estimated using deep dives and excluded shallow resting dives, allowing us to use the same coefficients for resting dives. Several individuals (11/42) had to be excluded from the simulation because tissue density could not be estimated as a result of an insufficient number of gliding periods or the lack of seawater density estimates (Burslem et al., 2025).

As the surface area (A) and mass (m) of each individual were unknown (apart from the individuals shown in Table S3), the diving gas volume (V_{air}) and the drag coefficient (C_d) were treated as combined terms, as respectively the diving gas volume per unit mass (V_{air}/m) and the combined drag term ($C_d{\cdot}A/m$). Air volume values were converted from standard reporting units (ml kg^{-1}) to SI units (m^3 kg^{-1}) by applying a correction factor of 10^{-6}. The population estimate of the combined drag term of $9.59{\cdot}10^{-6}$ m^2 kg^{-3} was used for all individuals (Miller et al., 2004; Burslem et al., 2025). Individual estimates were used for tissue density.

Estimation of the onboard gas volume

Empirical estimates from the analyses described above were specified for all the parameters of Eqns 1–5 except for the diving gas volume during the resting dive. The simulation was therefore used to estimate the onboard gas volume during resting dives. To specifically test how bubbles modulated buoyancy, resting dives were subdivided into segments between bubble releases. For each of these segments, the simulation was used to estimate the onboard gas volume that best replicated the depth profile of each segment.

The beginning of the dive was defined as the first time point when individuals had a steep head-down position, characterised by an absolute pitch angle steeper than −75 deg, and when the depth recorded by the tag was at least 10 m deep, to ensure that the entire body of the whale was submerged. The end of the resting dive was characterised as the last time point when the whale had a steep head-up position (pitch ≥+75 deg). The period of time during rotation from a head-down to a head-up position was excluded from the simulation as the drag term is expected to change during that period. Rotation was defined as the period taken for the pitch to pass from −75 deg to +75 deg plus neighbouring periods where the rate of pitch rotation exceeded 0.3 deg s^{-1}. [Note, for some head-down/head-up resting dives, no head-down periods were selected as the individuals did not have a pitch steeper than −75 deg and a depth greater than 10 m. For these individuals, the beginning of the rotation was set to −75 deg.]

Segments shorter than 25 s were excluded from the simulation as depth changes during this short time period were not large enough to materially influence diving gas volume estimates. Moreover,

periods with sudden changes in pitch (s.d.≥4.9 deg over 15 s) were excluded as sudden changes in pitch would affect the drag force as a result of changes in the surface area. Periods during which depth data indicated that the head of the whale could have reached the surface were also excluded.

In order to estimate the onboard gas volume, the simulation aimed to mimic the depth profile of each segment. To do so, the velocity (smoothed using a 4 s moving average) and depth of the first time point of the segment were taken from the biologging data as starting points (Fig. 3). The simulation generated time series for the estimated acceleration, velocity and depth throughout each segment's duration. The simulation was run over a wide range of plausible diving gas volumes from 2 to 30 ml kg^{-1} with intervals of ±0.0001 ml kg^{-1}. As an adult male sperm whale of 15 m is estimated to weigh about 36 tons (mass=1.10×19.6×$length^{2.74}$, where mass is in kg and length is in m; 19.6 is an allometric scaling factor and 1.10 accounts for blood loss when whales are weighed in pieces; Lockyer, 1991), the precision of the total diving gas volume would be within millilitres. The best-fitting onboard gas volume was determined as the simulated gas volume that led to the smallest difference from the final depth of the segment (Fig. 3). Only segments with a final depth difference smaller than 50 cm between the simulation and recorded depth for head-down/head-up resting dives, and smaller than 150 cm for deep drifting resting dives were retained for further analysis. The best onboard gas volume was then saved for each segment. For each segment, the goodness of fit was estimated via a root mean squared error (RMSE) of the depth contour. These errors excluded the first and last time point of the segment, as the first one was taken from the biologging data and the last one was selected to be the closest to the data.

Fluking detection

Segments were inspected for fluking using body rotations estimated from magnetometer data (Martín López et al., 2022). For each individual, a body rotation magnitude threshold (in radians) was defined to detect strokes (Burslem et al., 2025).

Statistical analysis

All statistical analyses were performed in the RStudio statistical programming environment (https://posit.co/). To test for a negative monotonic relationship between the estimated onboard gas volume and the segments predicted by our hypothesis, Spearman rank correlations were performed for each resting dive. To test whether there was a common relationship for all the resting dives, generalised estimating equations (GEEs) were applied to account for the longitudinal structure of the data. GEEs were implemented using the function geeglm in the geepack package (Højsgaard et al., 2006) with a Gaussian family and an autoregressive (AR-1) working correlation structure. Segment number was used as the explanatory variable, and the interaction between individual whale identifier and dive number was specified as the clustering factor to account for repeated measures within individuals and dives. A natural logarithm was applied to diving gas volume to improve normality. A finite-sample bias-corrected sandwich variance estimator (fij correction) was used to adjust for the low number of clusters (N=10). Models were applied only to head-down/head-up resting dives owing to the small sample size of deep drifting resting dives. The estimated diving gas volumes of each individual between foraging and resting dives were compared using a paired t-test. Finally, to test the relationship between the depth and the velocity at the time of bubble releases, a Pearson correlation test was performed. All values are presented as means±s.d., except when noted otherwise. The threshold for statistical significance was set at P=0.05.

RESULTS

Resting dives

Of the 42 tagged individuals, 17 were recorded resting. Among the individuals that rested, the total duration of resting ranged from 7 min to over 3 h (mean±s.d. duration 68.4±56.7 min). Resting accounted for an average of 9.2±9.0% of the duration of tag deployments (minimum 1.0%, maximum 29.1%), and the number of resting dives ranged from 1 to 8 (3.6±2.3). The duration of resting dives ranged between 6 and 31 min (19.0±6.5); however, it is worth noting that the minimal duration of a resting dive was constrained by the selection criterion that resting dives should be longer than 5 min.

The same three ways of resting described in the Introduction ('head-up', 'head-down/head up' and 'deep drifting') were found in the dataset (Fig. 4). Isojunno and Miller (2015) only included in the last of these category classifications resting dives that happened after a period of foraging. However, in this study, any deep resting dives with descent parts not classified as resting were classified as deep drifting dives. Individual sw09_141a had three resting dives

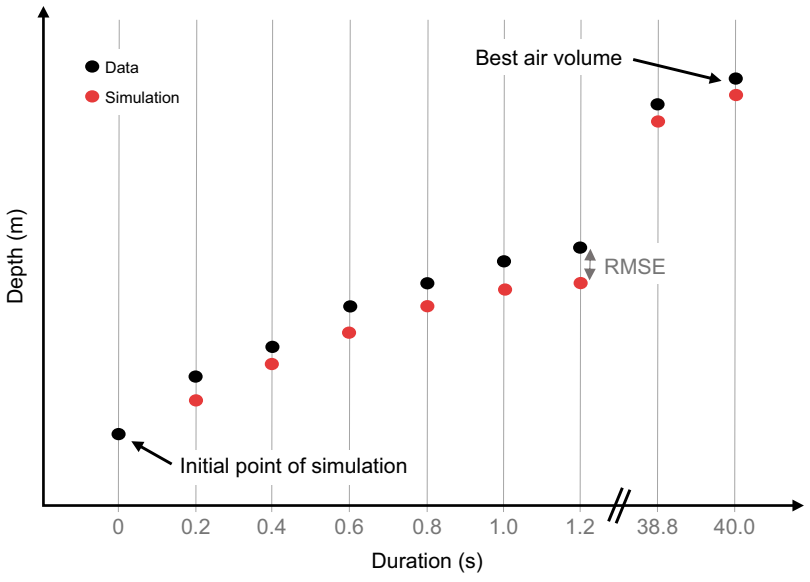

Fig. 3. Conceptual illustration of the implementation of the simulation on a segment. The simulation was run with 0.2 s intervals. The initial velocity and depth of the simulation were taken from the data. The best onboard gas volume is considered to be the one that minimises the error between the final depth of the data and the final depth estimated by the simulation. The root mean squared error (RMSE) between the simulated and actual depth was calculated for each segment to estimate the goodness of fit.

Journal of Experimental Biology (2026) 229, jeb251920. doi:10.1242/jeb.251920

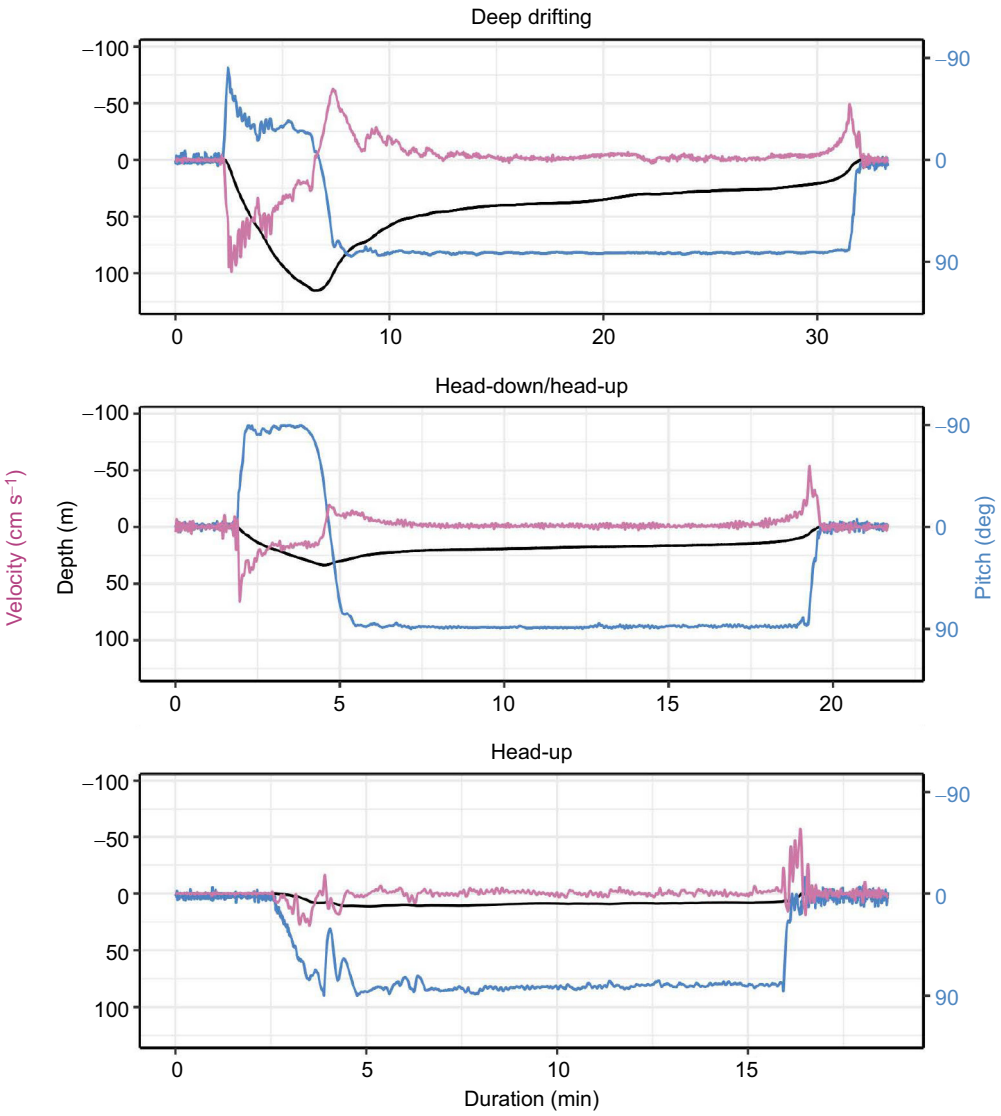

Fig. 4. The three different types of resting dives observed in the data. Depth is in black, velocity is in pink and pitch is in blue. Deep drifting dives represent resting dives where individuals drifted up to the surface after a dive (ID: sw09_142a). Head-down/head-up dives represent resting dives where whales first dived in a head-down position before reversing into a head-up position (ID: sw10_147a). Head-up resting represents resting dives where individuals go straight into a head-up position (ID: sw17_179a).

during which it seemed to be resting for a short period just before reversing into a head-up position; however, these short moments of resting were preceded by heavy fluking and happened at great depth (>150 m); they were therefore classified as deep drifting (Fig. 4; e.g. Fig. S35). Echolocation clicks were heard on the descent part of most of these deep drifting dives (75%).

During deep drifting, individuals started drifting at an average depth of 203.6±107.2 m, while individuals resting during head-up resting dives started drifting at an average depth of 8.1±4.1 m (not accounting for the distance from the rostrum to the tag), and individuals resting during head-down/head-up resting dives started at an average depth of 27.5±11.9 m.

Among the 17 individuals that rested, 9 rested only during head-down/head-up dives, 3 rested only during head-up dives and 2 rested during deep drifting dives (Table S1). The 3 remaining individuals rested in two different ways: 2 individuals rested during head-up and head-down/head-up dives, and 1 individual rested during head-down/head-up and deep drifting dives (Table S1). Within the dataset, head-down/head-up resting dives were the most common way for sperm whales to rest (60% of individuals; Table S1).

Bubble releases

For 91.8% of all the resting periods (56 out of 61 resting periods), releases of bubbles were heard. The remaining five resting dives for which no bubble releases were heard were either head-up resting dives close to the surface, very deep drifting (>200 m) or deep drifting dives where fluking was detected.

The duration of bubble releases had an average duration of 7.8 ±5.8 s (minimum 0.3 s, maximum 32.7 s). The number of release events per dive ranged from 0 to 36 (7.9±7.3 bubble releases). Head-down/head-up dives had the most bubble releases with an average of 10.9±7.5 (minimum 1, maximum 36). Head-up dives had an average number of bubble releases of 2.0±1.6 (minimum 0, maximum 5) and deep drifting dives had an average number of bubble releases of 3.5±4.1 (minimum 0, maximum 11).

Simulation performance

For the majority of segments (89.4%), the simulation provided a satisfactory fit with low associated errors (terminal error <50 cm for head-down/head-up and <150 cm for deep drifting resting dives). The mean RMSE was 0.4±0.7 m for head-down/head-up and 2.6±3.1 m for deep drifting resting dives. For both types of resting

dives, RMSEs were positively correlated with the duration of the 166 segments (Pearson correlation coefficient, r_{166}=0.81, P<10^{-15}).

Diving gas volume at the start of resting dives

The average tissue density of the individuals was 1029.6±0.9 kg m^{-3} (Burslem et al., 2025), and the estimated seawater density between 0 and 100 m for all the deployments was 1027.0±0.3 kg m^{-3}. Diving gas volume estimates indicated that individuals carried 8.0±1.6 ml kg^{-1} of diving gas at the start of head-down/head-up resting dives, significantly lower than the 26.4±3.9 ml kg^{-1} estimated for foraging dives (Miller et al., 2004; Burslem et al., 2025; Fig. 5; paired t-test, t_9=18.6, P≤10^{-5}) and corresponding to a total diving gas volume of 234 l for an individual weighing 30 tons.

The simulation was also applied to two individuals resting during deep drifting resting dives (Table S2). Diving gas volume before any bubble releases could only be estimated for one of the two individuals (sw09_141a). The estimated diving gas volume was 27.9±3.0 ml kg^{-1}, which was greater than the diving gas volume estimated for head-down/head-up resting (8.0±1.6 ml kg^{-1}) and more similar to the diving gas volume estimated for foraging dives (26.4±3.9 ml kg^{-1}). For the other individual, sw09_142a, the diving gas volume could only be estimated after a bubble release and the estimated diving gas volume was 12 ml kg^{-1}, suggesting that for this individual the initial diving gas volume was closer to the diving gas volume of head-down/head-up resting dives. The two deep drifting resting dives of individual sw09_142a were atypical, with a substantial initial ascended distance (>35 m) and a subsequent decrease in vertical velocity (Figs S39 and S40).

Regulation of buoyancy via bubble releases

A negative monotonic relationship was found between the estimated diving gas volume and the head-up segment number within all head-down/head-up resting dives, indicating that the resulting diving gas volume decreased across segments (Table 2, Figs S1–S40; Spearman rank correlations). This negative relationship was found for all the resting dives for which it could be calculated (resting dives with at least two head-up segments). Similarly, GEE analysis across all whales found a significant relationship between the segment number and the diving gas volume (Wald statistic=51.5, P<10^{-12}), with an average difference of −5.2% in diving gas volume between segments (Fig. S1), supporting the hypothesis that the whales reduced their diving gas volume to maintain their position in the water column.

In contrast to the observed dives, a depth profile simulated with an onboard gas volume fixed to that in the previous segment led to rapid ascent, causing the head-up period to be drastically reduced in duration relative to the observed dives and simulations in which onboard gas volume was estimated to have decreased (Fig. 6). A negative monotonic relationship was also found between onboard gas volumes and segment numbers of deep drifting resting dives (Table S2; Spearman rank correlation). Although a decreasing trend was found for both types of resting, there were a few cases (10.4% of the head-up segments) where the estimated diving gas volume was lower than that of the following segment.

DISCUSSION

Despite variation in the number of bubble releases among individuals, all sperm whales tagged in this study released bubbles during head-down/head-up resting dives. Some individuals seemed to achieve near-neutral buoyancy via relatively few bubble releases, while others released bubbles throughout the resting dive. There was no indication that the number of bubble releases during a heads-down resting dive was related to animal tissue density (Table 2). However, as we were not able to estimate the rate of gas discharge during individual release events, the number of release events does not necessarily correspond to total air volume released or deviation from neutral buoyancy. In contrast, head-up resting dives exhibited fewer bubble releases, possibly associated with limitations of detectability or because, by not swimming underwater, these individuals were not aiming to achieve a specific position in the water column. In the context of deep drifting resting dives, releases of bubbles varied considerably from one resting dive to another. In cases where resting dives started at depths exceeding 100 m, the number of bubble releases decreased. This suggests that these individuals did not need to modulate buoyancy via bubble release to rest long enough because of the greater ascent distances.

A physical simulation was created and used to investigate the role of bubble releases, which highlighted a decrease in the onboard gas volume throughout resting dives, indicating active control of onboard gas volumes to control net buoyancy. Whales also began their resting dives with a smaller initial diving gas volume relative to foraging dives, suggesting they were planning to rest in the dive and needed less diving gas as a result. The simulations demonstrated satisfactory reproduction of the majority of the tested segments, unlike alternative simulations assuming a fixed diving gas volume, which deviated markedly from the observed dive profile data (Fig. 6). This study therefore provides a detailed description of the influence of net buoyancy on resting sperm whales and supports the hypothesis that sperm whales use bubble releases to regulate their net buoyancy.

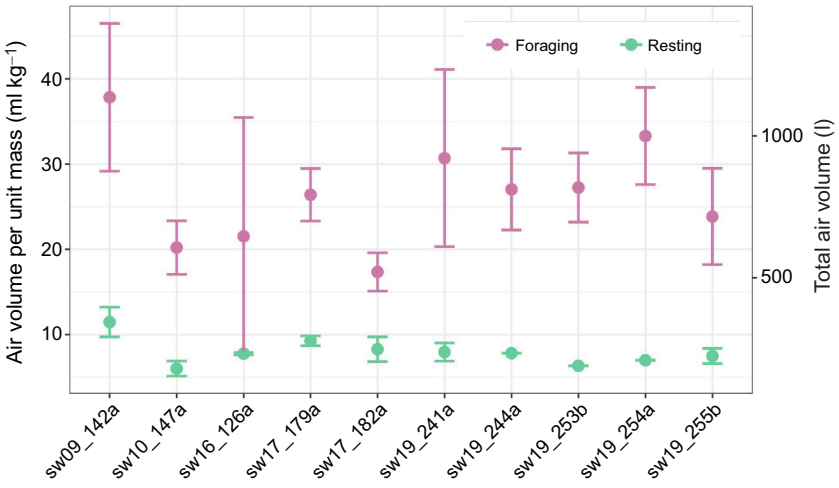

Fig. 5. Estimated gas volume per unit mass for foraging and resting dives for each individual. The equivalent total gas volume of an individual of 30 tons (14 m long) is shown on the right *y*-axis. Gas volume data are estimates±s.d.

Table 2. Estimated diving gas volumes for head-down/head-up resting dives

					Volume of diving gas per unit mass (ml kg^{-1}) (RMSE)										
					Head-down segments	Head-up segments									
	Sperm whale ID	Tissue density (kg m^{-3})	Resting no.	No. of segments	1	1	2	3	4	5	6	7	8	9	Spearman correlation
1	sw09_142a	1030.085	1	10	12.704 (3.426)	16.368 (1.648)	13.914 (0.051)	14.170 (1.335)	12.637 (0.063)	12.106 (0.436)	11.554 (0.136)	10.898 (0.140)	9.740 (0.050)	9.363 (0.896)	−0.983
2	sw09_142a	1030.085	2	5	10.242 (0.274)	NA	10.132 (0.042)	NA	9.267 (0.738)						−1.000
3	sw10_147a	1028.816	1	8	4.585 (0.827)	6.028 (0.134)	4.760 (0.079)	4.603 (0.054)	4.444 (0.071)	4.057 (0.059)	4.155 (0.490)	3.671 (0.104)			−0.964
4	sw10_147a	1028.816	2	9	5.801 (1.312)	6.120 (0.067)	6.054 (0.219)	5.571 (0.046)	4.958 (0.048)	4.395 (0.135)	4.417 (0.117)	4.160 (0.074)	3.967 (0.065)		−0.976
5	sw10_147a	1028.816	3	5	5.881 (5.258)	5.266 (0.096)	5.020 (0.104)	4.776 (0.779)	3.530 (0.227)						−1.000
6	sw10_147a	1028.816	4	7	5.922 (1.180)	5.122 (1.214)	4.360 (0.056)	3.929 (0.155)	4.052 (0.075)	3.840 (0.199)	3.309 (0.093)				−0.943
7	sw10_147a	1028.816	5	8	5.729 (2.064)	6.286 (0.186)	5.403 (1.292)	4.799 (0.062)	4.570 (0.045)	4.238 (0.049)	4.195 (0.039)	3.590 (0.201)			−1.000
8	sw10_147a	1028.816	6	8	7.142 (0.720)	8.088 (0.297)	5.976 (0.045)	6.159 (0.078)	5.394 (0.983)	5.054 (0.109)	4.650 (0.061)	4.077 (0.156)			−0.964
9	sw10_147a	1028.816	7	7	7.106 (0.825)	7.154 (0.415)	6.013 (0.178)	5.447 (0.060)	5.075 (0.050)	4.827 (0.057)	4.254 (0.113)				−1.000
10	sw16_126a	1030.345	1	5	7.865 (0.757)	8.347 (0.439)	8.015 (0.451)	7.783 (0.240)	NA						−1.000
11	sw16_126a	1030.345	2	2	7.679 (1.131)	NA									NA
12	sw17_179a	1029.925	1	5	9.496 (0.110)	9.241 (0.387)	8.947 (0.133)	8.534 (0.093)	7.633 (0.068)						−1.000
13	sw17_179a	1029.925	2	4	8.522 (0.313)	8.413 (0.177)	7.921 (0.054)	7.383 (0.103)							−1.000
14	sw17_179a	1029.925	3	5	NA	10.681 (3.502)	8.154 (0.216)	8.236 (0.193)	7.585 (0.259)						−0.800
15	sw17_179a	1029.925	4	6	9.167 (0.357)	9.137 (0.312)	8.900 (0.077)	8.254 (0.075)	7.178 (0.091)	6.756 (0.123)					−1.000
16	sw17_179a	1029.925	5	6	NA	11.418 (1.686)	9.329 (0.139)	8.299 (0.083)	7.430 (0.087)	7.095 (0.149)					−1.000
17	sw17_179a	1029.925	6	6	NA	9.083 (0.677)	8.328 (0.055)	7.932 (0.061)	7.601 (0.287)	7.077 (0.128)					−1.000
18	sw17_179a	1029.925	7	9	9.908 (1.977)	11.066 (0.619)	9.325 (0.067)	9.433 (0.062)	9.453 (0.237)	9.045 (0.100)	8.866 (0.090)	9.123 (0.145)	8.900 (0.059)		−0.786
19	sw17_182a	1029.828	1	6	9.312 (0.342)	6.911 (0.545)	6.415 (0.172)	6.337 (0.309)	NA	NA					−1.000
20	sw17_182a	1029.828	2	2	7.267 (0.501)	NA									NA
21	sw17_182a	1029.828	3	9		5.729 (0.161)	5.766 (0.103)	5.590 (0.141)	NA	5.172 (0.102)	5.195 (0.089)	4.843 (0.309)	4.748 (0.121)	4.767 (0.122)	−0.929
22	sw19_241a	1029.999	1	6	8.718 (0.296)	8.305 (0.032)	8.610 (0.328)	7.643 (0.096)	7.627 (0.092)	NA					−0.800
23	sw19_241a	1029.999	2	1	7.205 (0.194)										NA
24	sw19_244a	1029.886	1	2		7.824 (0.829)	7.481 (0.121)								−1.000
25	sw19_244a	1029.886	2	2		7.835 (0.320)	7.545 (0.239)								−1.000
26	sw19_253b	1029.277	1	3	6.343 (0.415)	7.363 (2.397)	6.573 (0.417)								−1.000
27	sw19_254a	1028.749	1	2	6.992 (1.498)	8.164 (0.315)									NA
28	sw19_255b	1029.687	1	6	6.493 (0.733)	8.892 (1.424)	NA	7.207 (0.063)	6.716 (0.030)	NA					−1.000
29	sw19_255b	1029.687	2	4	NA	NA	NA	7.330 (0.087)							NA
30	sw19_255b	1029.687	3	6	7.812 (1.408)	8.928 (0.110)	NA	7.064 (0.276)	6.700 (0.088)	6.750 (0.172)					−0.800
31	sw19_255b	1029.687	4	1	8.187 (0.514)										NA

Data are estimates with RMSE in parentheses. Root mean squared error (RMSE) corresponds to the error between the depth profile of the simulation and the depth profile of the biologging data in meters. NA indicates segments for which the diving gas volume could not be estimated. The Spearman rank correlation between the estimated diving gas volume and head-up segments is indicated; NA represents cases where this could not be calculated (as a result of the number of head-up segments being lower than 2). The simulation was run with diving gas volumes to four decimal places, although they are displayed here using three decimal places for enhanced readability.

Journal of Experimental Biology (2026) 229, jeb251920. doi:10.1242/jeb.251920

Journal of Experimental Biology (2026) 229, jeb251920. doi:10.1242/jeb.251920

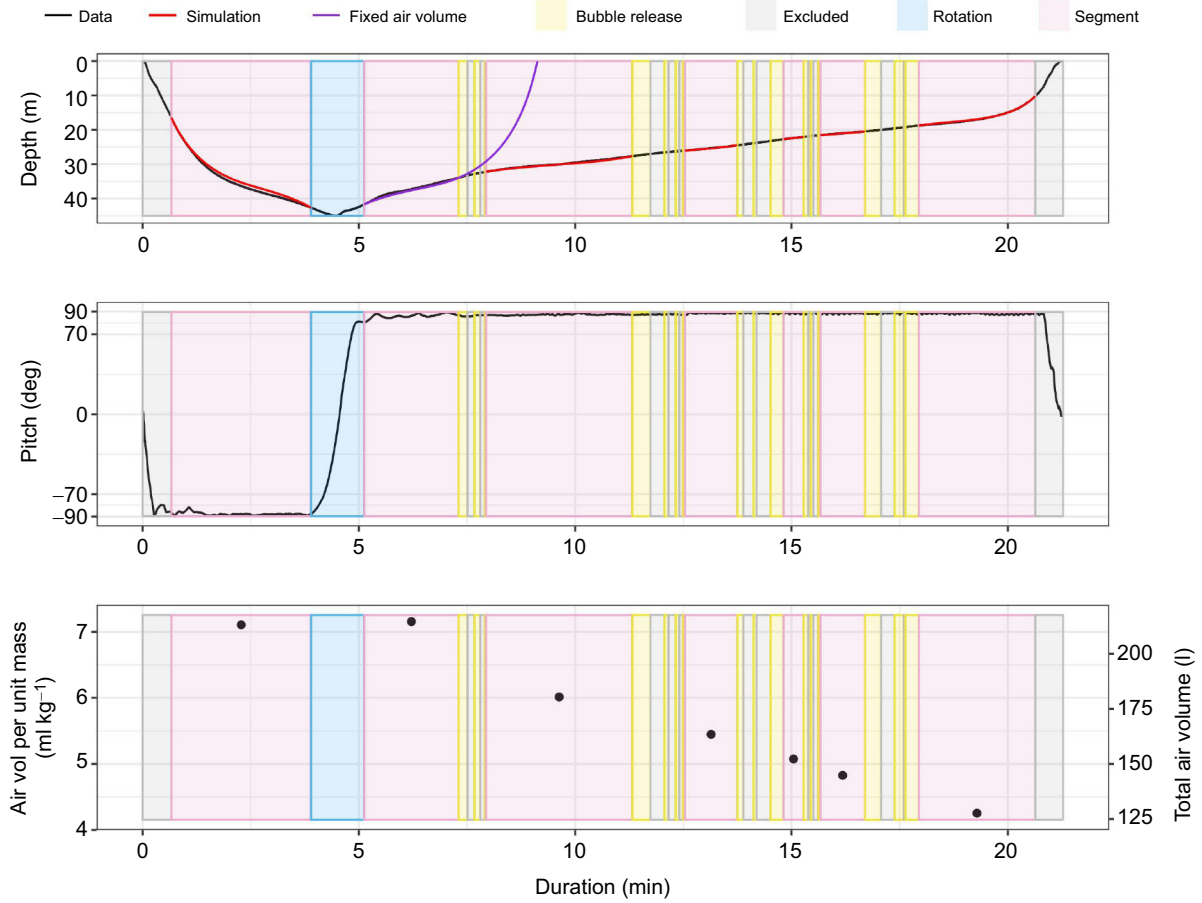

Fig. 6. Profile of the seventh resting dive of individual sw10_147a. Top: the depth profile of sw10_147a, with the simulation indicated in red and the data indicated in black. The purple line represents the depth profile with a fixed amount of gas. Middle: the pitch for each segment. Bottom: the estimated gas volume for each segment. Onboard gas volume is represented as gas volume per unit mass on the left *y*-axis; the equivalent in total gas volume, estimated for an individual of 30 tons (length of around 14 m), is shown on the right *y*-axis. The different shading indicates the different parts of the dive: rotation (blue), excluded parts of resting dives (light grey), bubble releases (yellow) and segments (pink).

Although examples of buoyancy regulation mechanisms exist in the literature, only two other species have been documented to release bubbles specifically for this purpose. Grey whales (*Eschrichtius robustus*), for example, appear to strategically release bubbles to extend foraging dives, particularly in more buoyant individuals (Bird et al., 2024). Similarly, bowhead whales (*Balaena mysticetus*) were shown to release bubbles during drift dives, which was also hypothesised to aid buoyancy regulation (Blackwell et al., 2022). Other marine species also release bubbles for functions other than buoyancy regulation. Humpback whales (*Megaptera novaeangliae*) and bottlenose dolphins (*Tursiops truncatus*), for instance, appear to blow bubbles for purposes of prey capture and apparent play (Friedlaender et al., 2011; McCowan et al., 2000), respectively. These behaviours are inconsistent with observed sperm whale bubble releases, which occur mainly during resting dives. Antarctic fur seals (*Arctocephalus gazella*) also release bubbles, but continuously during ascent (Hooker et al., 2005). In this case, exhalations are thought to help seals prevent shallow-water blackouts rather than maintain neutral buoyancy. Unlike fur seals, sperm whales release bubbles intermittently and primarily during resting dives, suggesting that the functional roles differ between the two species.

Results from the simulation indicated that sperm whales take less diving gas for head-down/head-up resting dives than for foraging dives, suggesting that sperm whales adjust their diving gas volume depending on the type of dive. This finding was supported by footage of sperm whales filmed immediately before and after resting dives (Movies 2 and 3). In the footage, sperm whales seem to exhale diving gas before diving head down without inhaling and do not seem to exhale after the resting dive once they reach the surface. The diving gas volume brought from the surface varied across individuals (s.d.=1.6 ml kg^{-1}) and showed greater consistency among dives of the same individual (s.d.=0.9 ml kg^{-1}).

Modification of diving lung volume has been reported for king penguins (*Aptenodytes patagonicus*) and Adélie penguins (*Pygoscelis adeliae*), and southern elephant seals (*Mirounga leonina*), which modulate inspired diving gas volume to optimise buoyancy (Sato et al., 2002, 2025). Because of the shallow depths of head-down/head-up resting dives, sperm whales would need less diving gas to remain neutrally buoyant near the surface. In contrast, foraging dives require more diving gas to support echolocation (Madsen et al., 2002), whereas shallow resting dives generally lack click production. For deep drifting resting dives, the estimated diving gas volume appeared greater than for head-down/head-up resting dives in at least one individual (sw09_141a). This may reflect the greater maximum depths of deep drifting dives, as a larger diving gas volume would be needed to achieve passive upward drift. Furthermore, in dives which immediately preceded drifting, sperm whales (including sw09_141a) typically produced echolocation clicks, requiring a sufficient amount of diving gas.

While our results indicate that presence and timing of bubble releases suggest they are used to maintain neutral buoyancy, it does

not necessarily follow that this represents the only function of bubble releases during resting. It is possible that release of dissolved CO_2 and N_2 gases from blood and tissues could increase the volume and mixture of gases in the lungs. Indeed, resting near the surface would reduce partial pressure of those gases in the lungs, enabling more effective diffusion from the blood into the lungs and thus facilitating the release of slower-diffusing gases that might build up over multiple deep foraging dives. This potential function of bubble release would not affect our biomechanical conclusions as we neither measured the volume of gas released as bubbles nor assumed that inspiration before diving is the only possible gas input. Rather, our analysis indicates that the amount of gas retained in the body following each bubble release (regardless of any other inputs or outputs) diminished over the course of resting dives in a manner consistent with the maintenance of neutral buoyancy. Further research could assess this possible function more directly. For example, to test this possibility empirically, our methodology could potentially be extended to compare water column position and velocity against expected gas kinetics as predictors of bubble release timing.

Methods considerations

Some minor potential indications of potential fluking motions were visible in the rotations signal during resting, predominantly occurring during the descent or just after the rotation. Fluking during descent could allow sperm whales to rest deeper, while fluking during ascent may happen when individuals 'overshoot' their depth of neutral buoyancy. We therefore conclude that minor exceptions to the overall excellent fit between simulated and measured depth data may have been influenced by the length of the segments and the potential presence of minor stroking movements (that were below the threshold to detect fluke strokes). Such missed stroking could also introduce minor discrepancies between estimated diving gas volume before and after the rotation, resulting in respective underestimations and overestimations. However, we concluded that as any such stroking events were limited to a few isolated, transient cases and were of insufficient amplitude to be detected using established methods, they are unlikely to have affected our overall conclusions. Differences in gas volume estimates before and after body rotation could arise from the lung being higher in the water column after rotation (see 'Location of the centre of rotation' in Supplementary Materials and Methods). The vast majority of the biologging data was collected in the context of sonar experiments. Such sonar exposure may have altered the behaviour of the whales to some extent; however, the mechanisms of buoyancy regulation should not have been affected as they reflect physical processes.

Another methodological limitation of our study includes our reliance on acoustic data alone. While efforts were made to thoroughly examine bubble releases and include only high-quality data, some faint releases may not have been audible, or other signals may have been mistakenly labelled as bubble releases. While inaudible releases are likely to be small and therefore exert relatively minor influences on the whale's body, future studies could involve video-recording tags placed close to the blowhole of sperm whales, to improve bubble release detectability and positively confirm their occurrence from acoustic scoring (Nazario et al., 2022).

By releasing bubbles, sperm whales appear to actively regulate their position in the water column while resting. These actions indicate a certain level of awareness of the environment to gauge when adjustments to their net buoyancy are needed. However, it is unknown whether the release of bubbles is a conscious process. Because of feasibility issues, the brain activity of resting sperm whales has not been measured; it remains, therefore, unknown whether they sleep unihemispherically or bihemispherically. If sperm whales sleep unihemispherically, buoyancy regulation could be overseen by the awake hemisphere; however, such regulation might also be compatible with bihemispheric sleep. Videos capturing both eyes of resting sperm whales could help to shed light on which of these forms of sleep they use. Similarly, it remains unknown what cues (e.g. lung volume versus vertical speed) prompt the animals to release bubbles. Future work comparing the predictions of alternative potential cues with observed data could help to shed light on the cues used and in turn the level of awareness likely to be necessary for buoyancy regulation. Ultimately, improved insights into the awareness level of sperm whales while resting near the surface could potentially have important implications for their vulnerability to anthropogenic threats such as ship strikes.

While head-down/head-up resting dives appeared, from the dataset, to be the most prevalent way of resting, sperm whales also rested during head-up and deep drifting resting dives. Although head-down/head-up resting dives seem to grant a greater buffering from whale surface action than head-up resting dives, it remains unclear why some individuals rested while drifting up from substantial depths. An advantage associated with deep drifting could be a reduced need for active buoyancy regulation. The fact that certain individuals exhibit more than one resting behaviour suggests that environmental conditions or internal state might influence the type of resting dive. For example, the type of resting dive might also depend on their body condition, particularly for individuals with less buoyant tissues, for which neutral buoyancy at depth would be hard to achieve (Miller et al., 2004). Humpback whales (*M. novaeangliae*) were also shown to rest in two ways: while logging at the surface or drifting up from greater depths (Iwata et al., 2021). It was hypothesised that the use of one of the two ways of resting depends on several conditions, such as sea state, body density and buoyancy. The motivations underlying the selection of a given resting behaviour in sperm whales could potentially be investigated using longer tag deployments covering a greater range of internal and environmental states.

Conclusions

Our study demonstrates active buoyancy regulation in resting sperm whales, achieved through bubble release and a reduction of surface-borne gas volumes throughout resting dives. Release of bubbles was found to mechanistically predict their ability to maintain near-neutral buoyancy at a shallow depth during resting dives. These results highlight the important role of buoyancy in the resting behaviour of sperm whales, illustrate the diverse strategies they employ to achieve extended periods of resting, and indicate the extent to which they are able to gauge their environment and optimise their behaviour during this time. If the whales are indeed sleeping during these resting periods, our findings indicate that they are capable of fine positioning control even during sleep. To explore this question further, it would be interesting to confirm sleep during these periods using novel EEG tags, and to identify the precise cues used by the whales to determine when to release gases.

APPENDIX

The hydrodynamic performance equation

Eqn A1 is the original equation for hydrodynamic performance by Miller et al. (2016):

$$a = -\frac{1}{2}\cdot\frac{C_{\mathrm{d}}\cdot A}{m}\cdot\rho_{\mathrm{sw}}\cdot v^2 + \left(\frac{\rho_{\mathrm{sw}}}{\rho_{\mathrm{tissue}}} - 1\right)\cdot \boldsymbol{g}\cdot\sin(p) + \frac{V_{\mathrm{air}}}{m}\cdot\boldsymbol{g}\cdot\sin(p)\cdot\frac{(\rho_{\mathrm{sw}} - (\rho_{\mathrm{air}}\cdot(1+0.1\cdot d)))}{(1+0.1\cdot d)}. \quad \text{(A1)}$$

For a detailed description of the abbreviations, see Table 1.

Compressibility of the tissue

Eqn A2 is the equation describing the compressibility of the tissue by Miller et al. (2016):

$$\rho_{\text{tissue}}(d) = \frac{\rho_{\text{tissue}}(0)}{1 - r \cdot (1 + 0.1 \cdot d) \cdot 101,325 \cdot 10^{-9}}. \quad \text{(A2)}$$

ρ_{tissue} corresponds to the tissue density, r to the whale tissue compressibility factor (value of 0.386; Burslem et al., 2025), d to the depth and 101,325 to a constant to convert pressure in atmospheres into Pascals.

Bubble auditing

Bubble releases vary substantially in both duration and intensity. The intensity of the bubble releases was assessed by looking at the colour on the spectrogram, with warmer colours indicating greater sound intensities. A typical event of bubble release comprises a loud period of clustered bubbles followed by a period of fainter and sparser bubbles. The variation in sound intensity and spacing suggests that during the initial part, air is forcefully expelled from the blowhole and that during the second part, the open blowhole allows bubbles to escape. Some bubble release events did not start with an initial loud release of bubbles and instead only consisted of faint and sparse bubbles. Discrete bubble releases were defined as bubble releases separated by intervals exceeding 2 s. Notably, instances with drastic increases in sound intensity were categorised as a new bubble release, regardless of the interval.

Acknowledgements

Thanks to the multiple field teams and ships' crews that made this study possible. We would like to express our deepest gratitude to Prof. Klaus Zuberbühler for guidance, and Dan Costa for his feedback. We are also very thankful to Prof. Radu Slobodeanu for his help with the statistical analyses, in particular with the generalised estimating equations. We would like to kindly thank Patrick Dykstra for allowing us to use his footage to illustrate our findings.

Competing interests

The authors declare no competing or financial interests.

Author contributions

Conceptualization: N.F., A.B., P.J.O.M.; Data curation: A.B., P.J.O.M.; Formal analysis: N.F.; Funding acquisition: N.F., P.J.O.M.; Methodology: N.F., A.B., P.J.O.M.; Supervision: A.B., P.J.O.M.; Writing – original draft: N.F.; Writing – review & editing: N.F., A.B., P.J.O.M.

Funding

This work was supported by the Fonds des donations de l'Université de Neuchâtel. Fieldwork for data collection was supported by grants from the US Office of Naval Research, US Living Marine Resources Program (grant no. N39430–17-C-1935); the Ministerie van Defensie; the Defence Science and Technology Lab of the UK Ministry of Defence (grant no. DSTLX-1000137649); and the direction générale de l'armement (DGA) of the Ministère de la Défense (grant no. 1883003901).

Data and resource availability

Data reported in this article are available from the Open Science Framework (OSF): https://osf.io/xm5dt/. All other relevant data and details of resources can be found within the article and its supplementary information.

References

Arnold, G. P. and Geer Walker, M. (1992). Vertical movements of cod (*Gadus morhua* L.) in the open sea and the hydrostatic function of the swimbladder. *ICES J. Mar. Sci.* **49**, 357-372. doi:10.1093/icesjms/49.3.357

Bird, C. N., Pirotta, E., New, L., Bierlich, K. C., Hildebrand, L., Fernandez Ajó, A. and Torres, L. G. (2024). Bubble blasts! An adaptation for buoyancy regulation in shallow foraging gray whales. *Ecol. Evol.* **14**. doi:10.1002/ece3.70093

Biuw, M., McConnell, B., Bradshaw, C. J. A., Burton, H. and Fedak, M. (2003). Blubber and buoyancy: monitoring the body condition of free-ranging seals using simple dive characteristics. *J. Exp. Biol.* **206**, 3405-3423. doi:10.1242/jeb.00583

Blackwell, S. B., Tervo, O. M., Lemming, N. E., Quakenbush, L. T. and Heide-Jørgensen, M. P. (2022). Drift dives in a bowhead whale (*Balaena mysticetus*). *Aquat. Mamm.* **48**, 656-660. doi:10.1578/AM.48.6.2022.656

Burslem, A., Isojunno, S., Prieto, R., Silva, M. A. and Miller, P. J. O. (2025). Estimating lipid store mass *in-vivo* for free-ranging whales using drone photogrammetry and biologging tags. *Ecol. Evol.* **15**, e72472. doi:10.1002/ece3.72472

Clarke, M. R. (1978). Buoyancy control as a function of the spermaceti organ in the sperm whale. *J. Mar. Biol. Assoc. U. K.* **58**, 27-71. doi:10.1017/S0025315400024395

Flanigan, W. F. (1972). Behavioral states and electroencephalograms of reptiles. In *The Sleeping Brain: Perspectives in the Brain Sciences* (ed. M. H. Chase), pp. 14-18. Brain Information Service/Brain Research Institute, UCLA.

Friedlaender, A., Bocconcelli, A., Wiley, D., Cholewiak, D., Ware, C., Weinrich, M. and Thompson, M. (2011). Underwater components of humpback whale bubble-net feeding behaviour. *Behaviour* **148**, 575-602. doi:10.1163/000579511X570893

Højsgaard, S., Halekoh, U. and Yan, J. (2006). The R Package geepack for generalized estimating equations. *J. Stat. Softw.* **15**, 1-11. doi:10.18637/jss.v015.i02

Hooker, S. K., Miller, P. J. O., Johnson, M. P., Cox, O. P. and Boyd, I. L. (2005). Ascent exhalations of Antarctic fur seals: a behavioural adaptation for breath-hold diving? *Proc. R. Soc. B* **272**, 355-363. doi:10.1098/rspb.2004.2964

Houser, D. S., Kvadsheim, P. H., Kleivane, L., Mulsow, J., Ølberg, R. A., Harms, C. A., Teilmann, J. and Finneran, J. J. (2024). Direct hearing measurements in a baleen whale suggest ultrasonic sensitivity. *Science* **386**, 902-906. doi:10.1126/science.ado7580

Isojunno, S. and Miller, P. J. O. (2015). Sperm whale response to tag boat presence: biologically informed hidden state models quantify lost feeding opportunities. *Ecosphere* **6**, 1-46. doi:10.1890/ES14-00130.1

Iwata, T., Biuw, M., Aoki, K., Miller, P. J. O. and Sato, K. (2021). Using an omnidirectional video logger to observe the underwater life of marine animals: humpback whale resting behaviour. *Behav. Process.* **186**, 104369. doi:10.1016/j.beproc.2021.104369

Johnson, M. P. and Tyack, P. L. (2003). A digital acoustic recording tag for measuring the response of wild marine mammals to sound. *IEEE J. Oceanic Eng.* **28**, 3-12. doi:10.1109/JOE.2002.808212

Johnson, M., Aguilar de Soto, N. and Madsen, P. (2009). Studying the behaviour and sensory ecology of marine mammals using acoustic recording tags: a review. *Mar. Ecol. Prog. Ser.* **395**, 55-73. doi:10.3354/meps08255

Kendall-Bar, J. M., Williams, T. M., Mukherji, R., Lozano, D. A., Pitman, J. K., Holser, R. R., Keates, T., Beltran, R. S., Robinson, P. W., Crocker, D. E. et al. (2023). Brain activity of diving seals reveals short sleep cycles at depth. *Science* **380**, 260-265. doi:10.1126/science.adf0566

Kvadsheim, P. H., Lam, F. P., Isojunno, S., Wensveen, P. J., van IJsselmuide, S. P., López, L. M. M., Van Riet, M. W. G., McGhee, E. H., Siemensma, M. L., Bort, J. et al. (2020). Studying the effect of source proximity in sperm whales and continuous sonar in pilot whales using operational sonars. The 3S-2019-OPS Cruise Report. FFI-Rapport 2020. Kjeller: FFI.

Lam, F. P., Kvadsheim, P. H., Isojunno, S., Wensveen, P. J., van IJsselmuide, S., Siemensma, M., Dekeling, R. and Miller, P. J. O. (2018a). *Behavioral response study on the effects of continuous sonar and the effects of source proximity on sperm whales in Norwegian waters*. The 3S-2017 Cruise Report. TNO report TNO2018 R10958 (http://publications.tno.nl/publication/34627071/pohdo8/TNO-2018-R10958.pdf).

Lam, F. P., Kvadsheim, P. H., Isojunno, S., Wensveen, P. J., van IJsselmuide, S., Siemensma, M., Dekeling, R. and Miller, P. J. O. (2018b). *Behavioural response study on the effects of continuous sonar on sperm whales in Norwegian waters*. The 3S-2016-CAS Cruise Report. TNO report TNO2018 R10802 (http://publications.tno.nl/publication/34627070/Q3bPWP/TNO-2018-R10802.pdf).

Lockyer, C. (1991). *Body Composition of the Sperm Whale, Physeter Catodon, with Special Reference to the Possible Functions of Fat Depots*, Vol. 12, pp. 1-25. Marine Research Institute.

Madsen, P. T., Payne, R., Kristiansen, N. U., Wahlberg, M., Kerr, I. and Møhl, B. (2002). Sperm whale sound production studied with ultrasound time/depth-recording tags. *J. Exp. Biol.* **205**, 1899-1906. doi:10.1242/jeb.205.13.1899

Martín López, L. M., Aguilar de Soto, N., Madsen, P. T. and Johnson, M. (2022). Overall dynamic body acceleration measures activity differently on large versus small aquatic animals. *Methods Ecol. Evol.* **13**, 447-458. doi:10.1111/2041-210X.13751

McCowan, B., Marino, L., Vance, E., Walke, L. and Reiss, D. (2000). Bubble ring play of bottlenose dolphins (*Tursiops truncatus*): implications for cognition. *J. Comp. Psychol.* **114**, 98-106. doi:10.1037/0735-7036.114.1.98

Miller, P. J. O., Johnson, M. P., Tyack, P. L. and Terray, E. A. (2004). Swimming gaits, passive drag and buoyancy of diving sperm whales *Physeter macrocephalus*. *J. Exp. Biol.* **207**, 1953-1967. doi:10.1242/jeb.00993

Miller, P. J. O., Aoki, K., Rendell, L. E. and Amano, M. (2008). Stereotypical resting behavior of the sperm whale. *Curr. Biol.* **18**, R21-R23. doi:10.1016/j.cub.2007.11.003

Miller, P. J. O., Antunes, R., Alves, A., Wensveen, P. J., Kvadsheim, P. H., Kleivane, L., Nordlund, N., Lam, F.-P., van IJsselmuide, S., Visser, F. et al. (2011). *The 3S experiments: studying the behavioral effects of sonar on killer*

whales (Orcinus orca), sperm whales (Physeter macrocephalus), and long-finned pilot whales (Globicephala melas) in Norwegian waters. Scottish Ocean Inst. Tech. Rept. SOI-2011-001 (http://soi.st-andrews.ac.uk/documents/424.pdf).

Miller, P. J. O., Kvadsheim, P. H., Lam, F.-P. A., Wensveen, P. J., Antunes, R., Alves, A. C., Visser, F., Kleivane, L., Tyack, P. L. and Sivle, L. D. (2012). The severity of behavioral changes observed during experimental exposures of killer (*Orcinus orca*), long-finned pilot (*Globicephala melas*), and sperm (*Physeter macrocephalus*) whales to naval sonar. *Aquat. Mamm.* **38**, 362-401. doi:10.1578/AM.38.4.2012.362

Miller, P. J. O., Narazaki, T., Isojunno, S., Aoki, K., Smout, S. and Sato, K. (2016). Correction: body density and diving gas volume of the northern bottlenose whale (*Hyperoodon ampullatus*). *J. Exp. Biol.* **219**, 2962. doi:10.1242/jeb.148841

Millero, F. J. (2010). History of the equation of state of seawater. *Oceanography* **23**, 18-33. doi:10.5670/oceanog.2010.21

Moya-Laraño, J., Macías-Ordóñez, R., Blanckenhorn, W. U. and Fernández-Montraveta, C. (2008). Analysing body condition: mass, volume or density? *J. Anim. Ecol.* **77**, 1099-1108. doi:10.1111/j.1365-2656.2008.01433.x

Nazario, E. C., Cade, D. E., Bierlich, K. C., Czapanskiy, M. F., Goldbogen, J. A., Kahane-Rapport, S. R., van der Hoop, J. M., San Luis, M. T. and Friedlaender, A. S. (2022). Baleen whale inhalation variability revealed using animal-borne video tags. *PeerJ* **10**, e13724. doi:10.7717/peerj.13724

Piéron, H. (1913). *Le Problème Physiologique du Sommeil*. Paris: Masson et Cie.

Sato, K., Naito, Y., Kato, A., Niizuma, Y., Watanuki, Y., Charrassin, J. B., Bost, C.-A., Handrich, Y. and Le Maho, Y. (2002). Buoyancy and maximal diving depth in penguins. *J. Exp. Biol.* **205**, 1189-1197. doi:10.1242/jeb.205.9.1189

Sato, G., Adachi, T., Guinet, C. and Miller, P. J. O. (2025). Dive-by-dive variation in the diving respiratory air volume of southern elephant seals (*Mirounga leonina*). *J. Exp. Biol.* **228**, jeb249659. doi:10.1242/jeb.249659

Teloni, V., Mark, J. P., Miller, P. J. O. and Madsen, P. T. (2008). Shallow food for deep divers: dynamic foraging behavior of male sperm whales in a high latitude habitat. *J. Exp. Mar. Biol. Ecol.* **354**, 119-131. doi:10.1016/j.jembe.2007.10.010

Webb, P. M., Crocker, D. E., Blackwell, S. B., Costa, D. P. and Le Boeuf, B. J. (1998). Effects of buoyancy on the diving behavior of northern elephant seals. *J. Exp. Biol.* **201**, 2349-2358. doi:10.1242/jeb.201.16.2349

Highlighted Article: Tag data collected from sperm whales off the coast of Norway show that when they are resting, passively drifting below the sea surface, they actively regulate their buoyancy and vertical position by releasing bubbles.

Funding details

S.No.	Funder name	Funder ID	Grant ID
1	Université de Neuchâtel	http://dx.doi.org/10.13039/501100005353	
2	Office of Naval Research	http://dx.doi.org/10.13039/100000006	N39430–17-C-1935
3	Ministerie van Defensie		
4	Ministry of Defence	http://dx.doi.org/10.13039/100009941	DSTLX-1000137649
5	Ministère de la Défense	http://dx.doi.org/10.13039/501100005900	1883003901